

Nonlinear motion of coupled magnetic vortices in ferromagnetic/non-magnetic/ferromagnetic trilayer

**Su-Hyeon Jun¹, Je-Ho Shim¹, Subk-Kun Oh¹, Seong-Cho Yu¹, and Dong-Hyun Kim^{1a)},
Brooke Mesler^{2,3}, and Peter Fischer²**

¹Department of Physics, Chungbuk National University, Cheongju 361-763, South Korea

²Center for X-ray Optics, Lawrence Berkeley National Laboratory, Berkeley 94720, USA

³Applied Science and Technology Graduate Group, University of California at Berkeley,
Berkeley 94720, USA

Abstract

We have investigated a coupled motion of two vortex cores in ferromagnetic/non-magnetic/ferromagnetic trilayer cylinders by means of micromagnetic simulation. Dynamic motion of two vortex with parallel and antiparallel relative chiralities of curling spins around the vortex cores have been examined after excitation by 1-ns pulsed external field. With systematic variation in non-magnetic spacer layer thickness from 0 to 20 nm, the coupling between two cores becomes significant as the spacer becomes thinner. Significant coupling leads to a nonlinear chaotic coupled motion of two vortex cores for the parallel chiralities and a faster coupled gyrotropic oscillation for the antiparallel chiralities.

^{a)} Author to whom correspondence should be addressed. electronic mail: donghyun@cbnu.ac.kr

Recently, spin dynamics in confined geometry has attracted growing interest due to potential application of spintronics and magnetic storage in ferromagnetic nanoelements. It is well-known that magnetic vortex structure is formed in various confined geometries due to minimization of magnetostatic and exchange energies. Numerous studies have been devoted to understand the vortex structure [1] and dynamics [2-5]. In particular, understanding of magnetic vortex dynamics becomes more essential in the realization of nanometer scale spintronic devices and memory devices [6,7]. We know that a magnetic vortex is driven to move under an external magnetic field [2,8] or excited to move by a spin transfer torque [6]. The motion of vortex is known to be gyrotropic with circular trajectories in excited states [2,6,8]. Specific modes of gyrotropic vortex motion and relaxation in cylindrical dot was recently reported [4].

In the realization of spintronic and memory devices, multilayer structures are adopted for practical reasons. In the case of multilayers formed of ferromagnetic materials, multiple magnetic vortices may exist in a single magnetic element. Thus, understanding magnetic interaction between vortices in multilayer becomes important in technological application. Interaction between magnetic vortices was recently investigated for trilayer films with two ferromagnetic layers displaced by a non-magnetic spacer layer, where simulated motion of vortices is predicted to be similar to a damped simple harmonic oscillation with a weak coupling between two vortices [9]. However, no detailed study has been addressed to a strong interaction behavior between vortex cores in a multilayer system, while the interaction between vortex cores in a multilayer system becomes stronger as the system size becomes smaller down to nanometer scales.

In this work, we have carried out micromagnetic simulation study of coupled motion of vortices in the trilayer with systematic control of vortex chirality at the top and bottom layers as well as with variation in non-magnetic spacer layer thickness. It was observed that a chaotic coupled vortices motion clearly deviating from a damped simple harmonic oscillation appeared for the cases of same chiralities due to nonlinear vortex interaction in the trilayer. The coupling between two vortices becomes weak as non-magnetic spacer layer thickness becomes thicker, leading to a coupled simple damped harmonic oscillation.

We have carried out micromagnetic simulation using OOMMF [10] based on Landau-Lifshitz-Gilbert equation to investigate the coupled motion of vortices in a cylindrical ferromagnetic/non-magnetic/ferromagnetic trilayer film. In our simulation, material parameters of the ferromagnetic layers is chosen to be those of Permalloy with the exchange

stiffness coefficient of 13×10^{12} J/m and the saturation magnetization M_s of 8.0×10^5 A/m. The thickness of each Permalloy layer has been chosen to be 5 nm and the radius of the cylinder is set to be 250 nm. Spacer layer thickness is varied from 0 to 20 nm. Details of cylinder geometry are illustrated in Fig. 1. The cell size of micromagnetic simulation is $5 \times 5 \times 5$ nm³ and the damping constant is 0.03. Polarities of two vortices have been chosen to be the same with an upward direction as described in Fig. 1. The dynamic motion of two vortices with parallel and antiparallel relative chiralities has been examined under a pulsed external field. The width of the pulse field is 1-ns duration with a rising time of 0.1 ns and a falling time of 0.1 ns. Pulse with strength of 3.14 mT has been applied in the plane to excite vortices motion. Time-dependent vortices core positions are determined by processing and analyzing simulated images.

For comparison, we have investigated a case of the single layer without non-magnetic spacer, where the top (5 nm) and bottom (5 nm) Permalloy layers are in contact to each other, forming 10-nm Permalloy single layer. As the pulse field is applied, the vortex core has been kicked out of the equilibrium position at the center. Direction of the initial vortex core motion is determined by the torque originating from magnetization of the vortex core and curling spins around the vortex core. The field pulse is along the +x-direction, the vortex core magnetization is out of the plane along the +z-direction, and the curling spins around the core is clockwise, thereby the polarity (p) of the vortex is set to be '+1' and the chirality (c) '+1'. The torque exerted to the vortex core by the field is then along the -y-direction. The torque exerted to the curling spin on the left side of cylinder by the field is along the +z-direction, leading to the motion of the core along the -x-direction. Thus, an initial motion of the vortex core is toward the bottom left direction. Trajectory of the vortex core is illustrated on the top of Fig. 2. As demonstrated in the figure, the vortex core initially moves toward the bottom left due to the kick by the field pulse. After switching off the field pulse, the vortex core exhibits a gyrotropic motion with the counterclockwise sense of rotation determined by the handedness of the vortex structure[2,8].

Parallel and antiparallel relative chiralities of the bottom and top Permalloy layers are considered in the case with a non-magnetic spacer layer, where the top layer chirality is kept to be clockwise and the bottom layer chirality is varied to be either clockwise (parallel) or counterclockwise (antiparallel). As demonstrated in Fig. 2, the direction of initial motion of two vortex cores is same in the cases of parallel relative chiralities, whereas the direction becomes opposite in the cases of antiparallel relative chiralities. Although the initial motion depends on the handedness of vortex structure, the gyrotropic motion only depends on the

vortex core polarity so that two vortex cores exhibit the same sense of a counterclockwise rotation. In the case with a spacer layer thickness $d = 20$ nm, overall gyrotropic motions becomes similar irrespective of the relative chirality. However, in the case with a thinner spacer layer ($d = 5$ nm), a faster decaying behavior of the gyrotropic vortex core motion is vividly observed for an antiparallel relative chiralities as in the figure, which implies that there is a significant coupling phenomenon between two vortex cores of the top and bottom layers.

To investigate further details of coupling between two vortex cores, time-dependent vortex core positions of the top and bottom layers were analyzed, as shown in Fig. 3. Position of the vortex core along the y-axis is presented together with an average radial position and a lateral distance between two vortex cores with respect to time. The position of the core in all cases exhibits a damped oscillatory behavior. Although the initial radially kicked distance is almost the same within the error for both parallel/antiparallel chiralities cases, time evolution of average radial distances of parallel/antiparallel chiralities exhibits very striking difference with thinner spacer layers. In the case of antiparallel relative chiralities, oscillatory behavior decays faster as the spacer layer thickness becomes thinner. It becomes more evident by noting that an average radial distance and a lateral distance between two cores reach zero fastest when the spacer layer thickness is thinnest ($d = 5$ nm). This can be explained by taking into account the fact that a mutual interaction of two cores on the bottom and top layers is attractive. Since two cores have the same polarities ($p = +1$), they prefer to have shortest lateral distance between them due to the flux closure of the core magnetization. The effective attractive force between two cores becomes stronger with the thinner spacer layer so that the oscillation decays faster, as demonstrated in Fig. 3.

In the case of parallel chiralities, a faster decay of an oscillatory behavior doesn't exist, since there is no attractive force between the two cores across the disk, as seen in the figure. If there is no coupling between the two cores, lateral distance between them will be zero all the time. However, even when the spacer layer is thickest ($d = 20$ nm), the lateral distance is not zero all the time but oscillating although the amount of oscillation of the lateral distance is relatively small. Thus, we cannot neglect coupling effect of the two cores in all cases. The lateral distance deviates further from zero with the thinner spacer layer. Very interestingly, when $d = 5$ nm, the coupled oscillation behavior survives longest as the average radial distance accordingly survives longest. Moreover, it should be noted that oscillatory behavior of the two cores becomes chaotic after about two cycles of gyrotropic motion. During the chaotic coupled motion, the lateral distance between the two cores becomes even greater than

the average radial distance. Considering the interaction between the two cores is always attractive, it seems that a strong non-linear interaction plays a key role in the chaotic motion regime.

Coupled oscillatory behavior with variation of the spacer layer thickness has been fitted, as demonstrated in the Fig. 4. Vortex core position projected onto the y-axis is fit at the time when the pulse field is switched off ($t = 1$ ns). For comparison, a simple gyrotropic motion of the single layer vortex has been fit with a damped simple harmonic oscillation motion as $y = y_0 \exp(-\beta t) \sin(\omega_0 t)$, where $y_0 = -41.7$ nm, $\beta = 6.9 \times 10^7$ s⁻¹, and $\omega_0 = 1.1 \times 10^8$. The simple fitting is matching well as shown in the top of the figure. In the case of thicker spacer layer ($d = 20$ nm), very weak coupling resulted in almost independent gyrotropic motions of two vortices irrespective of relative chiralities. Thus, the position of each vortex core is still fit with a damped simple harmonic oscillatory motion, as demonstrated in the bottom of Fig. 4.

Chaotic motion of the vortex core due to the significant attractive interaction for the case of thinner spacer layer ($d = 5$ nm) is explainable based on a simple model. We assume that each vortex core with M_z component as a magnetic dipole \vec{m}_{vortex} and estimate dipole-dipole interaction energy to be $\frac{\mu_0}{4\pi r^3} (3(\vec{m}_{\text{vortex}1} \cdot \vec{u}_{12})(\vec{m}_{\text{vortex}2} \cdot \vec{u}_{12}) - \vec{m}_{\text{vortex}1} \cdot \vec{m}_{\text{vortex}2})$, where μ_0 is the permeability, r is the interdistance between two dipoles, and \vec{u}_{12} is a unit vector along the direction of the relative displacement of two dipoles. The lateral attractive force is then the derivative of the energy with respect to s , the lateral displacement between two dipoles, where $r = \sqrt{s^2 + d^2}$ for the non-magnetic spacer layer thickness d . The force $f(s)$ is found to have a form of $f(s) = \frac{A \cdot s(-1 + B \cdot s^2)}{(1 + C \cdot s^2)^{7/2}}$ with fitting parameters A , B , and C . The attractive force is used as a weak coupling force in the simultaneous differential equations of two weakly coupled damped simple harmonic oscillators. By numerically solving the simultaneous differential equation with proper selection of fitting parameters, we could successfully reproduce the chaotic motion of coupled vortices, as demonstrated in Fig. 4 ($A = 1.5 \times 10^{19}$, $B = 1.0 \times 10^{16}$, and $C = 4.0 \times 10^{16}$). The chaotic behavior after few initial oscillations is qualitatively reproduced for the trilayer with 5-nm spacer thickness in the cases of parallel chiralities and the faster oscillation of vortex core with a shorter lateral distances between two cores are observed as well in the cases of antiparallel chiralities. Fitted curves with the same fitting parameters are plotted as well for the other chirality and other spacer layer thickness in Fig. 4.

In conclusion, the motion of vortices in ferromagnetic/non-magnetic/ferromagnetic trilayer cylinders have been systematically investigated with the variation in the thickness of non-magnetic spacer layer from 0 to 20 nm as well as with variation in the relative chiralities of curling spins on the top and bottom ferromagnetic layers. Vortex cores on the top and bottom layers exhibit gyrotropic motion, which becomes significantly coupled for the spacer layer thickness less than 10 nm. It has been found that, in the coupled motion regime, an attractive coupling force due to the magnetostatic interaction between two cores leads to the faster gyrotropic oscillation in the cases of the antiparallel chiralities and even to nonlinear chaotic motion in the cases of the parallel chiralities.

This work was supported by the Korea Research Foundation Grant funded by the Korean Government (Grant No. KRF-2007-331-C00097). This work was supported by the Director, Office of Science, of the US Department of Energy under contract No. DE-AC02-05CH11231.

References

- [1] M. Bode *et al.*, Phys. Rev. Lett. **100**, 029703 (2008).
- [2] S. B. Choe *et al.*, Science **304**, 420 (2004).
- [3] K. Y. Guslienko *et al.*, J. Appl. Phys. **91**, 8037 (2002).
- [4] K. Y. Guslienko, Appl. Phys. Lett. **89**, 022510 (2006).
- [5] Ki-Suk Lee *et al.*, Phys. Rev. B **76**, 174410 (2007).
- [6] K. Yamada *et al.*, Nature Mater. **6**, 270 (2007).
- [7] H.-G. Piao *et al.*, Appl. Phys. Lett. **94**, 052501 (2009).
- [8] B. Van Waeyenberge *et al.*, Nature **444**, 461 (2006).
- [9] K. Y. Guslienko *et al.*, Appl. Phys. Lett. **86**, 223112 (2005).
- [10] M. J. Donahue and D. G. Porter, OOMMF User's Guide: <http://math.nist.gov/oommf> (2002).

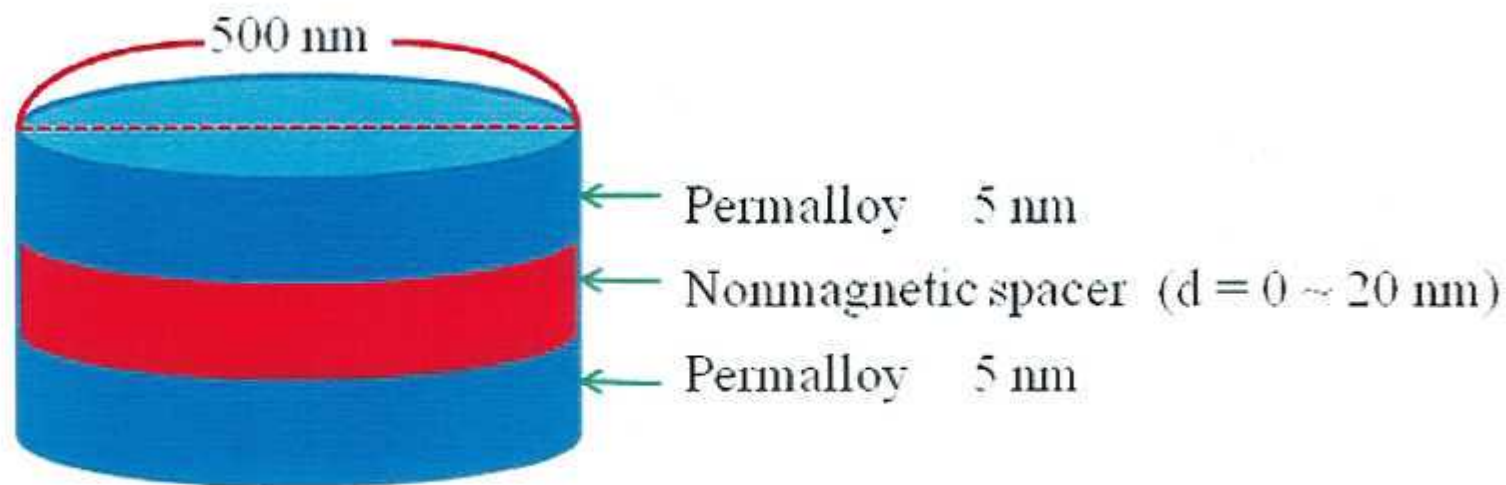
Figures

Figure 1: (a) Schematic diagram of a trilayer cylinder structure. (b) Parallel relative chiralities of curling spins on the top (clockwise) and bottom (clockwise) layers. (c) Antiparallel relative chiralities of curling spins on the top (clockwise) and bottom (counterclockwise) layers.

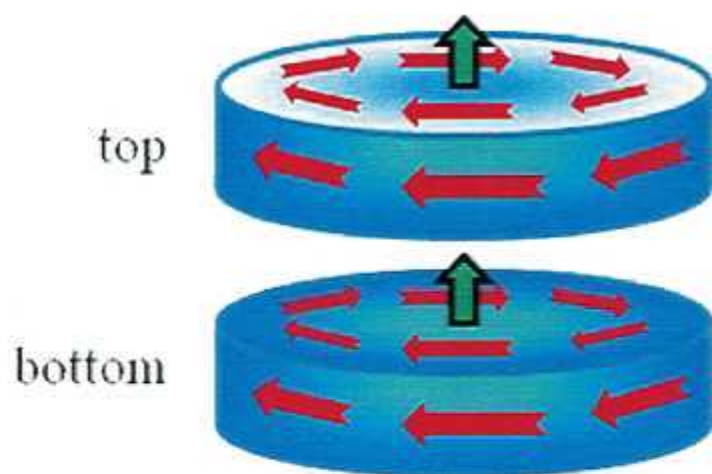
Figure 2: Time-resolved trajectories of vortices cores for different spacer layer thickness ($d = 5, 10, 15,$ and 20 nm) for parallel and antiparallel chiralities. Single layer case for $d = 0$ nm is shown on the top figure.

Figure 3: Vortex core position projected on the y-axis with respect to the time for different spacer layer thickness ($d = 5, 10, 15,$ and 20 nm), together with average radius of two cores from the center and lateral distance between two cores are plotted.

Figure 4: (a) Fitted motion of the vortex motion of the single layer ($d = 0$ nm) with a simple damped harmonic oscillation. (b) Fitted motion of coupled vortices cores for $d = 5$ nm in case of the parallel/antiparallel chiralities. (c) Fitted motion of coupled vortices cores for $d = 20$ nm in case of the parallel/antiparallel chiralities.

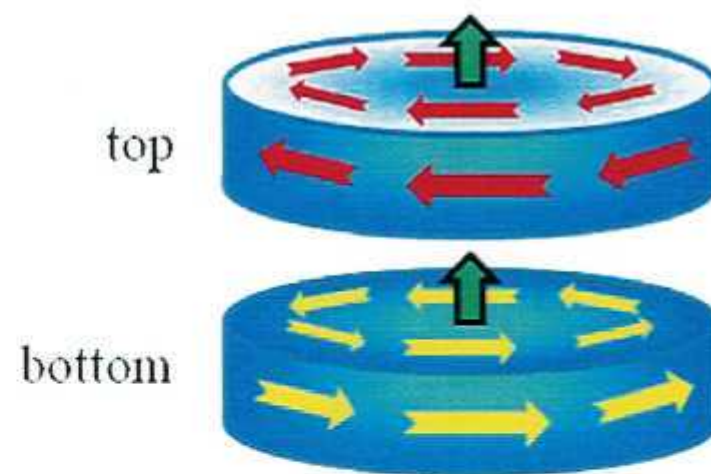


(a)



Parallel

(b)

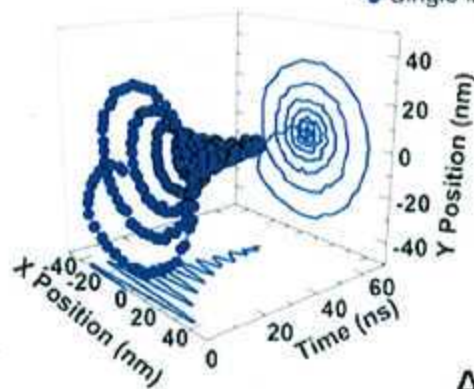


Antiparallel

(c)

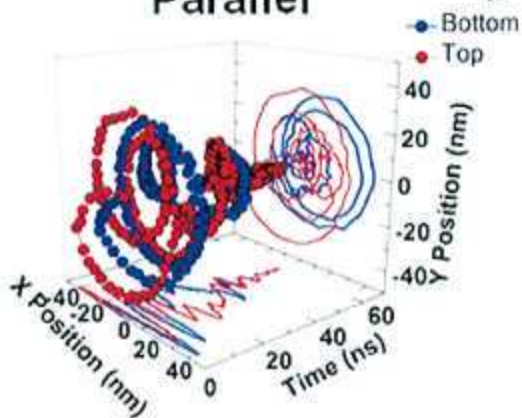
• Single layer

$d = 0$ nm

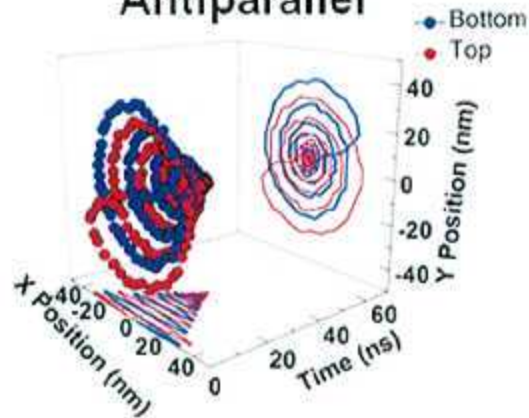


$d = 5$ nm

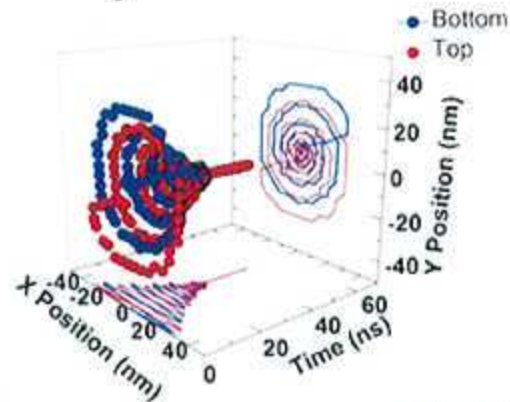
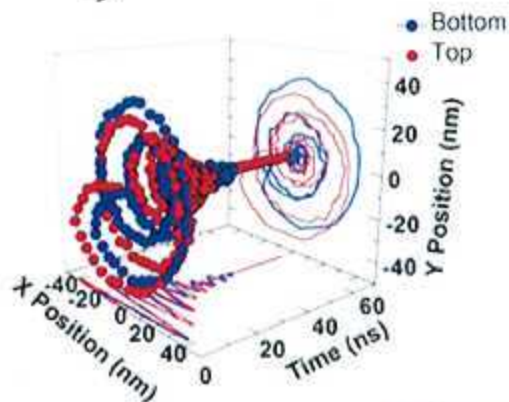
Parallel



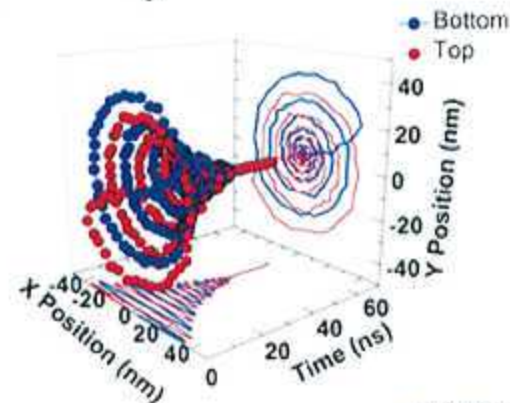
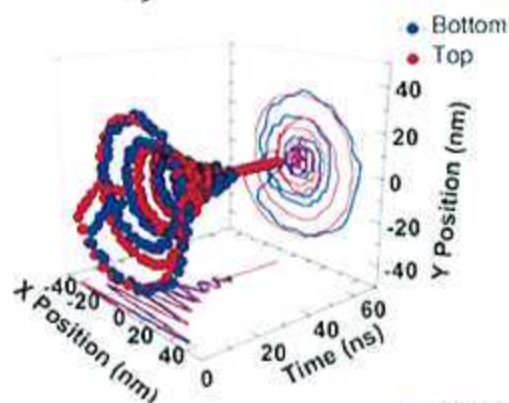
Antiparallel



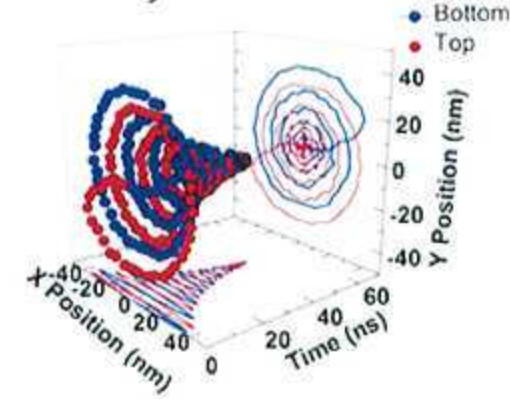
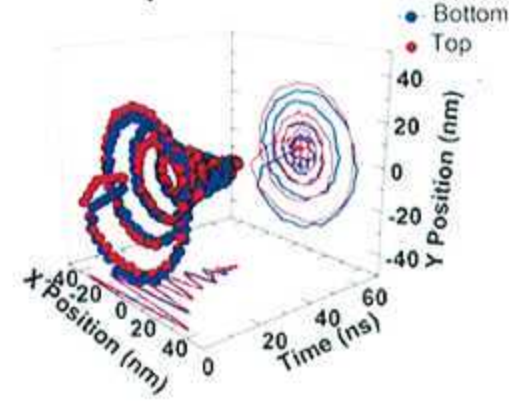
$d = 10$ nm



$d = 15$ nm

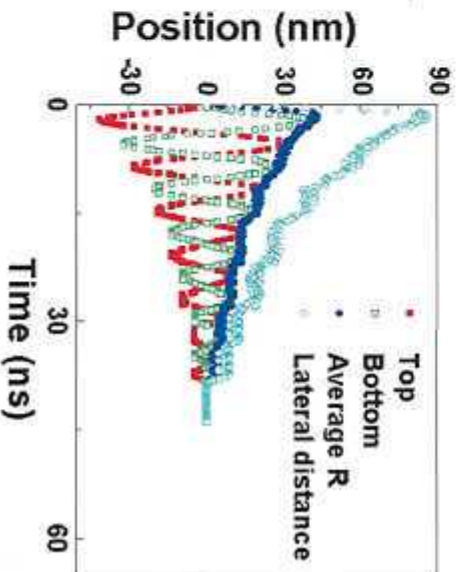
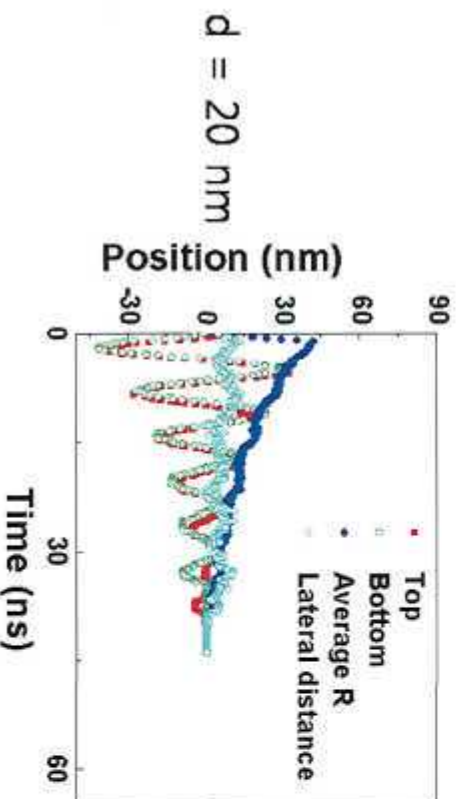
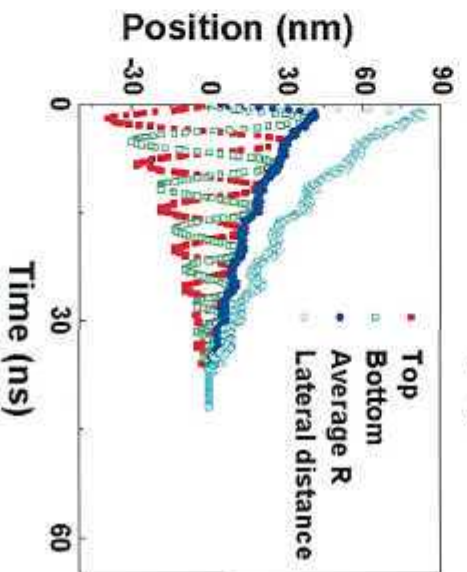
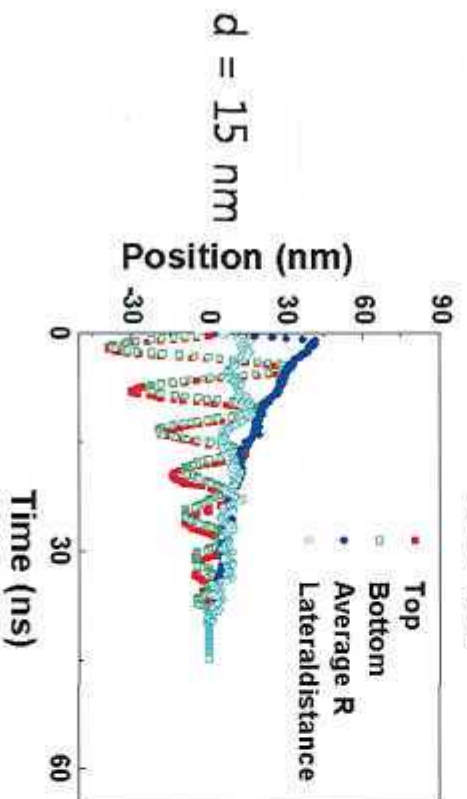
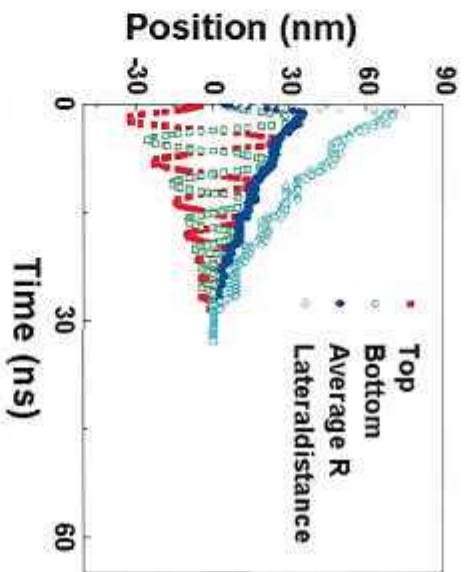
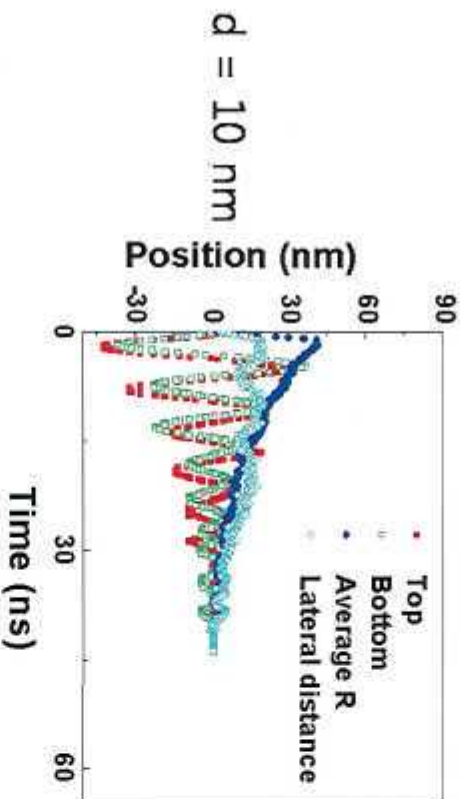
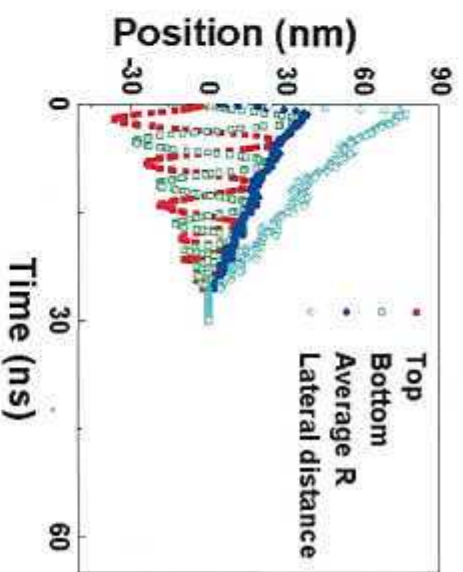
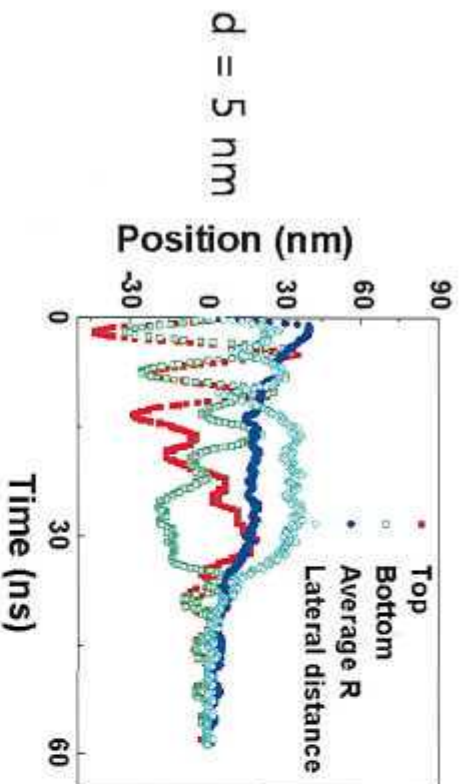


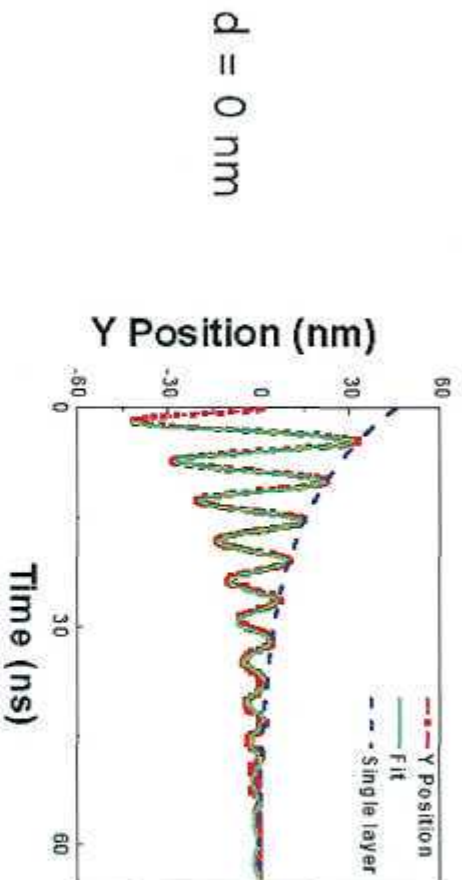
$d = 20$ nm



Parallel

Antiparallel

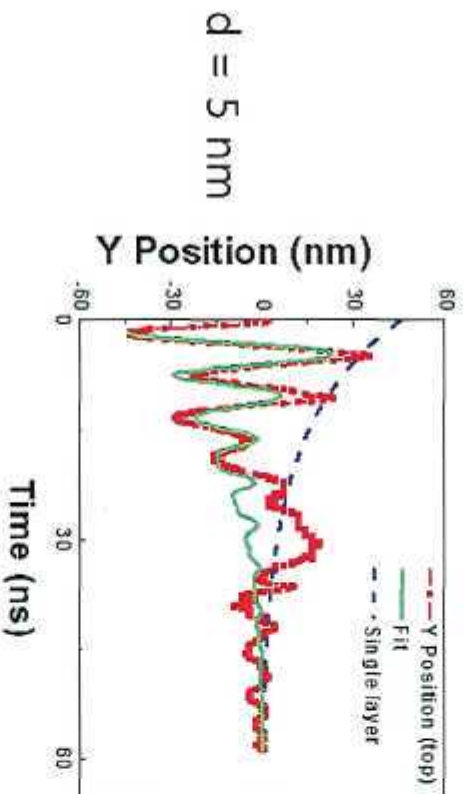




(a)

Parallel

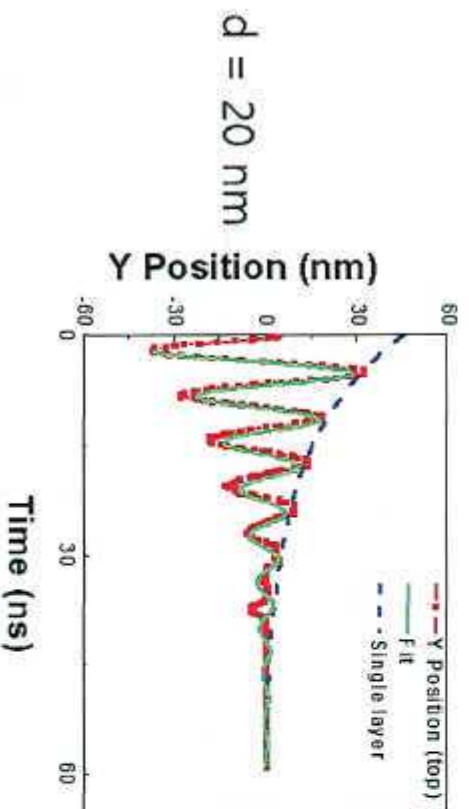
Antiparallel



(b)

Parallel

Antiparallel



(c)

